KEH-Gait: Towards a Mobile Healthcare User Authentication System by Kinetic Energy Harvesting

Weitao Xu[1,3], Guohao Lan[2,3], Qi Lin[2,3], Sara Khalifa[2,3], Neil Bergmann[1,3], Mahbub Hassan[2,3], Wen Hu[2,3]
[1]School of Information Technology and Electrical Engineering, University of Queensland, Australia
Email: {w.xu3}@uq.edu.au {n.bergmann}@itee.uq.edu.au
[2]School of Computer Science and Engineering, University of New South Wales, Australia
Email: {glan,sarak,mahbub,wenh}@cse.unsw.edu.au {qi.lin}@student.unsw.edu.au
[3]Data61 CSIRO, Australia

***Abstract*—Accelerometer-based gait recognition for mobile healthcare systems has became an attractive research topic in the past years. However, a major bottleneck of such system is it requires continuous sampling of accelerometer, which reduces battery life of wearable sensors. In this paper, we present *KEH-Gait*, which advocates use of output voltage signal from kinetic energy harvester (KEH) as the source for gait recognition. *KEH-Gait* is motivated by the prospect of significant power saving by not having to sample the accelerometer at all. Indeed, our measurements show that, compared to conventional accelerometer-based gait detection, *KEH-Gait* can reduce energy consumption by 78.15%. The feasibility of *KEH-Gait* is based on the fact that human gait has distinctive movement patterns for different individuals, which is expected to leave distinctive patterns for KEH as well. We evaluate the performance of *KEH-Gait* using two different types of KEH hardware on a data set of 20 subjects. Our experiments demonstrate that, although *KEH-Gait* yields slightly lower accuracy than accelerometer-based gait detection when single step is used, the accuracy problem can be overcome by the proposed Multi-Step Sparse Representation Classification (MSSRC). We discuss the advantages and limitations of our approach in detail and give practical insights to the use of KEH in a real-world environment.**

I. Introduction

With rapid advancements in embedded technology, wearable devices and Implantable Medical Devices (IMDs) have become an integral part of our everyday life. It is predicted that by 2025, the market for personal wearable devices will reach 70 billion dollar. The major deployments of those devices are expected to be in health monitoring and medical assistance domains [1], [2]. Some popular wearable devices, such as Fitbit and Apple Watch, are already monitoring and storing a mass of sensitive health data about the user. The private information of users can be further explored to provide a variety of emerging applications in the healthcare area. For example, the collected sensory data can be explored for the understanding of user's physical and mental health states [3].

Permission to freely reproduce all or part of this paper for noncommercial purposes is granted provided that copies bear this notice and the full citation on the first page. Reproduction for commercial purposes is strictly prohibited without the prior written consent of the Internet Society, the first-named author (for reproduction of an entire paper only), and the author's employer if the paper was prepared within the scope of employment.
NDSS '17, 26 February - 1 March 2017, San Diego, CA, USA
Copyright 2017 Internet Society, ISBN 1-891562-46-0
http://dx.doi.org/10.14722/ndss.2017.23023

However, such wearable systems are vulnerable to impersonation attacks in which an adversary can easily distribute his device to other users so that data collected from these users can be claimed to be his own. In this way, the attacker can claim potential healthcare profits that are allocated to people with certain illnesses even though he may not have any illnesses [4]. For instance, a policy holder may obtain a fraudulent insurance discount from a healthcare insurance company by using other people's health data. Another example is that in a mobile healthcare system for disease propagation control [5], an attacker can obtain additional vaccine allocation by launching user impersonation attacks and thus compromise the regular operations of such systems.

To mitigate the risk of malicious attacks, most wearable devices rely on explicit manual entry of a secret PIN number. However, due to the small screens of wearable devices and frequent unlocking requests, it is inconvenient for users to enter the keys manually. Furthermore, this method is not applicable when an adversary colludes with other users to spoof the healthcare company.

Gait recognition using wearable sensors, such as accelerometers, has emerged as one of the most promising solutions for user authentication. It offers several advantages over other biometrics especially when applied in wearables. For instance, although fingerprint and face have been proposed for user authentication on smartphones, fingerprint readers and cameras are not always available on wearable devices such as pacemakers and smart watches. In comparison, because walking is a daily activity, the main advantages of gait are its availability and spontaneity. Furthermore, gait is non-intrusive, and can be measured without subject intervention or knowledge [6]. This motivates us using gait as a biometric. Extensive previous studies have already demonstrated its feasibility in user authentication [7], [8], [9], but they have also shown that continuous accelerometer sampling drains the battery quickly. High power consumption of accelerometer sampling, which is typically in the order of a few milliwatts, also makes it challenging to adopt gait-based user authentication in resource-constrained wearables. Although power consumption may be not a big issue for wearables with large batteries such as smartphone, other wearables like IMDs suffer from short battery life because IMDs are long-lived devices and battery replacement requires surgical intervention [10].

A vision for wearable devices is to be battery-free (self-powered). A current trend in battery-free devices is to in-

vestigate kinetic energy harvesting (KEH) solutions to power the wearable devices [11], [12], [13], [14]. However, one fundamental problem in KEH is that the amount of power that can be practically harvested from human motions is insufficient to meet the power requirement of accelerometer for accurate activity recognition [15]. As reported in [11], the amount of power that can be harvested from human motion is only in the order of tens to hundreds of microwatts. This 2-3 orders of magnitude gap between power consumption and power harvesting is the biggest obstacle for realising gait-based authentication in batteryless wearables. Although the power consumption of sensors has been largely reduced in the last years thanks to the Ultra-Low-Power electronics [16], we believe in the near future energy harvesting will be used to augment or substitute batteries. For example, AMPY [17] has released the world's first wearable motion-charger which can transform the kinetic energy from user's motion into battery power. SOLEPOWER [18] produces smart boots that use user's steps to power embedded lights, sensors, and GPS. KINERGIZER has developed a small piezoelectric generator with the ability to harvest energy at low frequencies to produce as much as 200μW of power [19].

Motivated by this prospect, we propose gait recognition by simply observing the output voltages of KEH. The feasibility of the proposed idea is based on the observation that if humans have unique walking patterns, then the corresponding patterns of harvested power from KEH should be unique too. The proposed system offers several advantages. The major advantage of KEH-based gait recognition is the potential for significant power savings arising from not sampling accelerometer at all. On the other hand, the output voltage can be used to charge the battery, thus further extending battery life. Finally, as energy harvester will be integrated in wearable devices in the near future, the output voltage can be naturally utilized for authentication purpose without introducing extra sensors. This makes it a promising solution for light-weight authentication for wearable devices. The main challenge of implementing such a system is achieving high recognition accuracy by using a 1-axis voltage signal rather than 3-axis accelerometer signals. We address this issue by proposing a novel sparse fusion method which exploits the information from multiple steps. To the best of our knowledge, this is the first work that proposes and experimentally validates the feasibility of gait recognition using KEH. The main contributions of this paper are as follows:

- We propose a novel gait-based user authentication system for mobile healthcare system, called KEH-Gait, which uses only KEH voltage as the source signal to achieve user authentication.
- We build two different KEH prototypes, one based on piezoelectric energy harvester (PEH) and the other on electromagnetic energy harvester (EEH). Using these KEH devices, we evaluate gait recognition accuracy of KEH-Gait over 20 subjects. Our results show that, with conventional classification techniques, which operate over single step, KEH-Gait achieves approximately 6% lower accuracy compared to accelerometer-based gait recognition.
- We demonstrate that authentication accuracy of KEH-Gait can be increased to that of accelerometer-based gait detection by employing a novel classification method, called Multi-Step Sparse Representation Classification (MSSRC), which efficiently fuses information from multiple steps.
- Finally, using measurements, we demonstrate that currently available microprocessors can read KEH voltage within 33 μs, which is two orders of magnitude faster than what it takes to wakeup, interrogate and read acceleration values from typical 3-axis accelerometers. This means that with microprocessor duty cycling, KEH-Gait promises major energy savings over conventional accelerometer-based gait detection.

The rest of the paper is structured as follows. Sec II provides technical background on energy harvesting devices. Sec III introduces trust models and attacker models of gait-based authentication system. Sec IV presents the system architecture of KEH-Gait. Prototyping of KEH wearables and gait data collection are described in Sec V. We present evaluation results in Sec VI, and analyze power consumption in Sec VII. We have a discussion of our work in Sec VIII and introduce related work in Sec IX before concluding the paper in Sec X.

II. Background

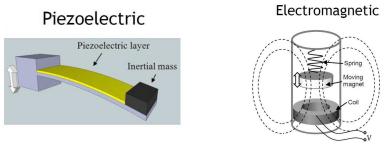

(a) (b)

Fig. 1: Examples of two KEH devices: (a) PEH, and (b) EEH.

Vibration-based energy harvesting has received growing attention over the last decade. The research motivation in this field is due to the reduced power requirement of small electronic components, such as the wireless sensor networks used in passive and active monitoring applications. The three basic vibration-to-electric energy conversion mechanisms are the piezoelectric [20], electromagnetic [21], [22] and electrostatic [23].

As electrostatic usually needs external voltage source, we built two proof-of-concept prototypes based on piezoelectric and electromagnetic respectively. Therefore, we briefly describe piezoelectric energy harvester (PEH) and electromagnetic energy harvester (EEH) to make the paper self-contained. The piezoelectric effect converts mechanical strain into electric current or voltage. This strain can come from many different sources, such as human motions and low-frequency seismic vibrations. Figure 1(a) shows a basic design of PEH. Piezoelectric vibrational energy harvesters are usually inertial mass based devices, where a cantilever with a piezoelectric outer layer is excited into resonance by a vibration source at the root of the cantilever. The inertial mass is located on a vibrating host structure and the dynamic strain induced in the piezoelectric layer results in an alternating voltage output. Unlike piezoelectric, the basic principle of electromagnetic generators are based on Faraday's law of electromagnetic induction. As shown in Figure 1(b), the voltage, or electromotive force is

generated when an electric conductor is moved through a magnetic field. Because of the small size and light weight, PEH is promising for hand-held and wearable devices such as wristwatches (e.g., the SEIKO Kinetic watch[1]), on the other hand, due to the weight of magnet, EEH usually has a larger weight and may not be embedded in the wearable devices, but can be used as an external mobile power source (e.g., the AMPY Move mobile charger).

III. Trust and Attack Models

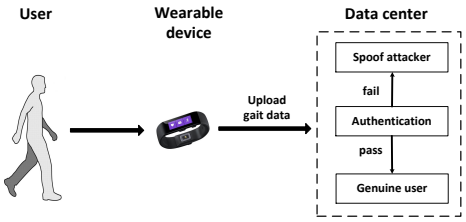

Fig. 2: The overview of a typical healthcare monitoring system.

We envision the use of KEH-Gait primarily in resource-constrained healthcare monitoring wearable devices to authenticate the identity of the user to prevent spoof attack. KEH-Gait addresses the issue of short battery life by using an energy harvester to replace an accelerometer. In the near future, energy harvesters can even be integrated in the hardware system to achieve battery-free wearable devices. Figure 2 illustrates the workflow of a typical healthcare monitoring system. In such a system, each user is given a unique user ID and a monitoring application which runs on a wearable device that can collect private sensor data and transmit them to the data centre of a healthcare company. Before transmission, the device first collects gait data and transmits them to the sever. The server will then perform authentication to verify the user's identity by using the gait data. If the user passes authentication, the further private data like blood pressure or heart rate are then transmitted to the server. While if the user verification fails, i.e., the user spoofing attack is detected, the sensor data collected from this user's device will not be reported to the server. In the server, sensor data will be analysed and processed by the healthcare company to derive user's physical and mental conditions. For instance, the measurements of heartbeats and blood pressure can be used to predict user's psychological conditions. A wide range of applications can also be enabled by such mobile healthcare systems and some examples are:

- User's physical behaviors are often reflection of physical and mental health and can be used by healthcare companies to facilitate early prediction of future health problems like depression [3].
- Health food companies can make advertisement by cooperating with healthcare related applications such as "IDOMOVE"[2], e.g., providing discount coupons for users who walk more than 1hr a day.

[1]KINETIC: http://www.seiko-cleanenergy.com/watches/kinetic-1.html.
[2]IDOMOVE: https://www.idomove.com/

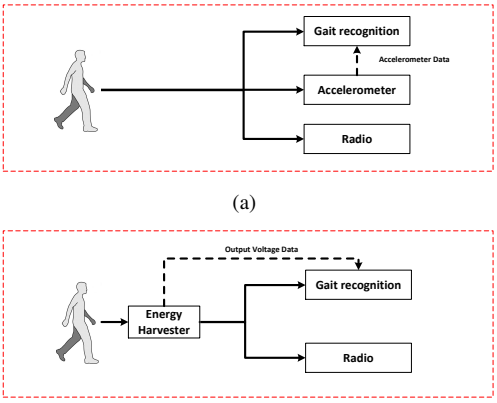

Fig. 3: Gait recognition systems: (a) conventional accelerometer-based gait recognition and (b) KEH-Gait.

For some applications, continuous authentication may be unnecessary. However, one-time validation of the users identity is becoming insufficient for modern devices and applications that process sensitive data. A simple example is the mobile phone will lock the screen and demand users to enter their PIN every few minutes. Such situations might benefit from a seamless authentication approach that incorporates continuous verification of the user's identity. KEH-Gait leverages gait which is a common daily activity to provide unobtrusive and continuous authentication without user intervention. There are also many commercial products that provide biometrics-based continuous authentication systems such as BehavioSec[3] and Eyefluence[4].

A. Trust Model

In this paper, we assume the data collected by sensors built in the wearable devices are trustworthy. Also, our system trusts the communication channel between the wearable device and the healthcare company's server. We discuss the feasibility of our assumption as follows.

Tamper-resistant Sensor. An attack can physically accesses to the sensor or chipset and manipulate the recorded data. To make sure the device has not been modified, a healthcare company can apply tamper-resistant techniques [24]. As mentioned in [25], ARM TrustZone extension can also be used to ensure the integrity of the sensors [26].

Trusted Transmission. A man-in-the-middle(MITM) attack may occur when the device is communicating with the server. Therefore, the device and server should establish a secure communication channel. To address this attack, the healthcare company can install a digital certificate in the wearable device and the device will perform SSL authentication when communicating with the server.

B. Attack Model

The aforementioned mobile healthcare system is vulnerable to user spoofing attacks. For instance, an adversary can distribute his device to another person, and upload the data of that person aiming to obtain healthcare benefits. Besides, multiple

[3]https://www.behaviosec.com/
[4]http://eyefluence.com/

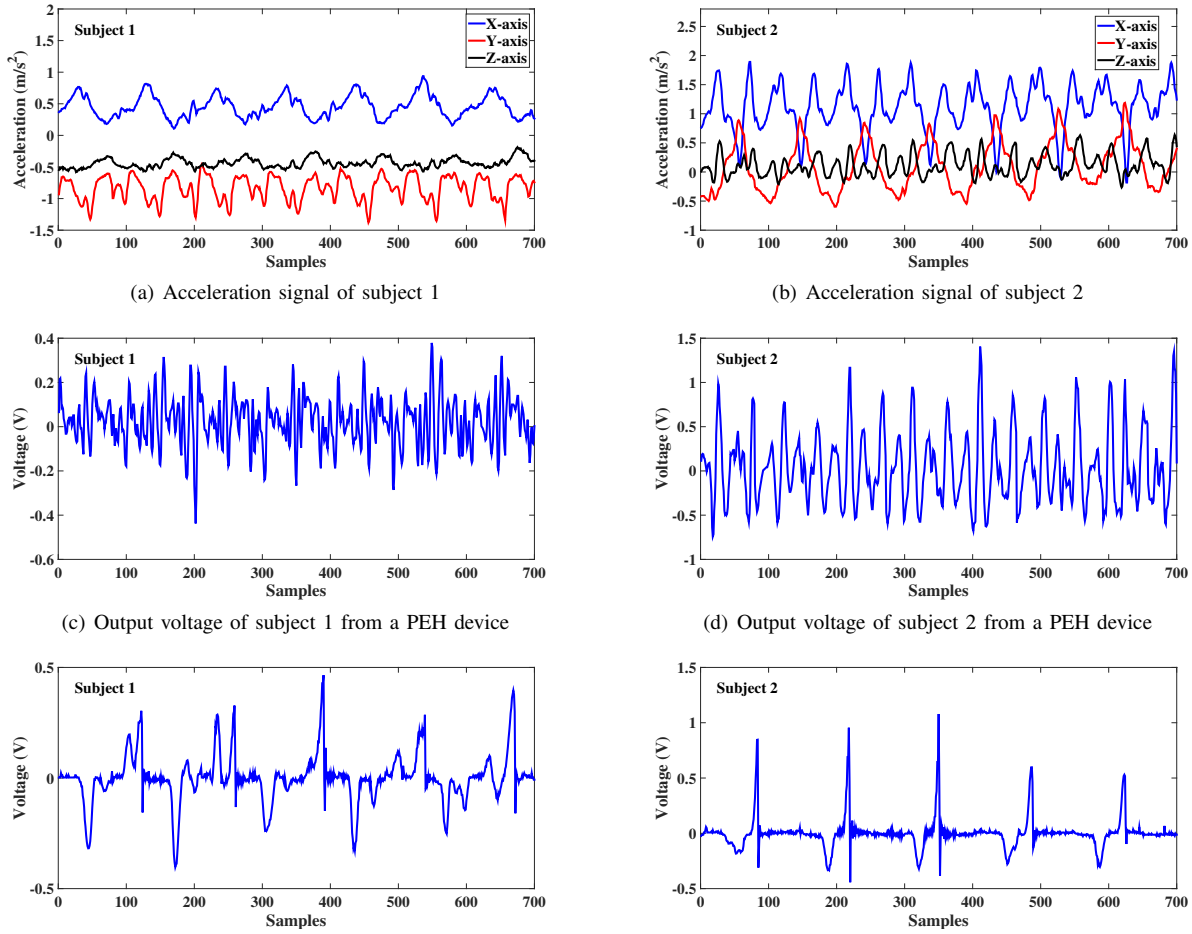

(a) Acceleration signal of subject 1

(b) Acceleration signal of subject 2

(c) Output voltage of subject 1 from a PEH device

(d) Output voltage of subject 2 from a PEH device

(e) Output voltage of subject 1 from an EEH device

(f) Output voltage of subject 1 from an EEH device

Fig. 4: A comparison of the output voltage signal from different devices: (a) and (b) exhibit the acceleration signal from 3-axis accelerometer when two different subjects are walking; (c) and (d) plot the output voltage signal from a PEH device; (e) and (f) show the output voltage signal from an EEH device.

users may collude to launch user spoofing attacks to fool the mobile healthcare system. Therefore, the adversary model considered in this paper focuses on impersonation attacks. We assume the presence of two types of impersonation attacks: a passive adversary and an active adversary. The passive adversary tries to spoof the healthcare system by using his own walking patterns. The active spoofing attacker knows the authentication scheme and will try his best to imitate the walking pattern of the genuine user to spoof the healthcare system.

The main goal of our system is to detect spoofing attacks. In fact, there are many other possible attacks to such healthcare system. We discuss these possible attacks and corresponding solutions. The first type of attacks we consider is replay attacks. In replay attacks, an adversary first records a measurement trace from another person. Then he replays the data trace to the monitoring device to fool the healthcare monitoring system. This attack can be easily detected as discussed in [25]. Although a MITM attack during communication between the device and server can be easily prevented, there is another type of MIMT in which an adversary may build a MITM monitor which bridges the user's skin and a wearable device. For example, once it detects a response message indicating healthy problems such as high blood pressure, it will manipulate the data and transmit the forged data to the server. This type of attack can be addressed by the scheme in [25]. Further potential threats include deriving the walking patterns by studying a video of the target's gait through computer vision techniques. We believe this is a potential vulnerability of unknown severity and leave it as future work.

IV. System Architecture of KEH-Gait

In this section, we discuss the proposed KEH-Gait framework in details. First, we compare KEH-Gait with traditional accelerometer based gait recognition system. Figure 3(a) shows the pipeline of a traditional accelerometer-based gait recognition system, in which the accelerometer data are used to train a classifier for gait recognition. In contrast, as shown in Figure 3(b), KEH-Gait exploits the output voltage signal of the kinetic energy harvester for gait recognition directly. By not using the accelerometer, KEH-Gait can save the energy that is used to sample the accelerometer. The saved energy can be further used to power other components in the wearable device, such as the classifier and radio. The radio can be used to transmit the personal data to a base station or a server.

Figure 4 compares the output voltage signal from two

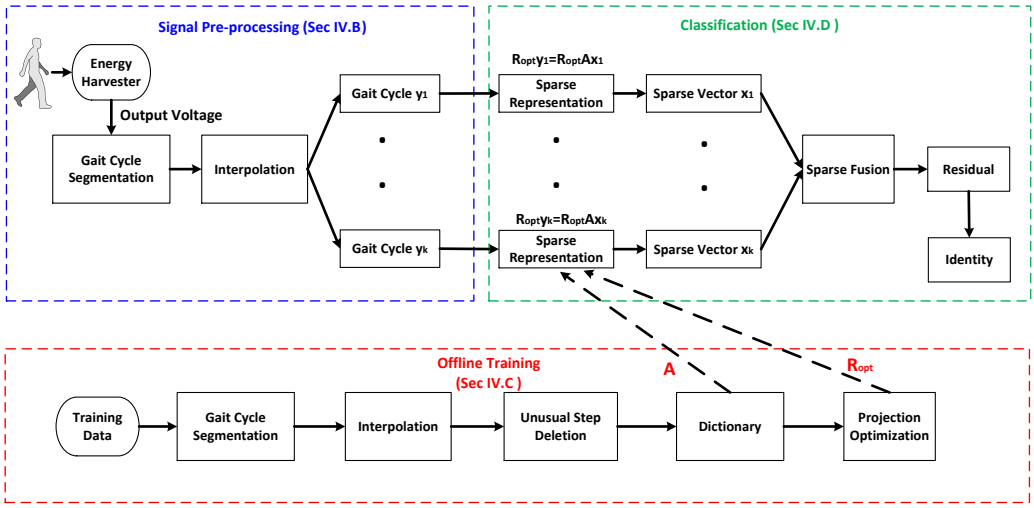

Fig. 5: System flowchart of KEH-Gait

types of energy harvester (EH) generated by two subjects when they are walking. These figures provide a clear visual confirmation that the voltage signal from the energy harvester contains personalized patterns generated by the subjects. This observation is promising as our goal is to recognize different subjects based on the output voltage signal of the EH when they are walking.

A. System Overview

As shown in Figure 5, the whole procedure of KEH-Gait consists of three parts: offline dictionary training, pre-processing of input signals, and classification.

During the offline dictionary training phase, gait cycles are first segmented from time series voltage signal and then interpolated into the same length. All detected cycles are passed to unusual cycles deletion to remove outliers of gait cycles. The obtained gait cycles are used to form the training dictionary A. After obtaining A, we apply the projection optimization algorithm in [27] to obtain a optimized projection matrix R_{opt}. Then the reduced training dictionary $\tilde{A} = R_{opt}A$ is used in the classifier as described in Section II.

After the acquisition of the test signal, we again apply gait cycle segmentation and interpolation to obtain the gait cycles from the test signal. The same optimized projection matrix (as used for training) is used to reduce the dimension of the test signal and provide the measurement vector $\tilde{y}_i = R_{opt}y_i$, $i = 1, 2, \cdots, k$, and k is the number of obtained gait cycles.

Now both the training dictionary $\tilde{A}$ and the measurements $\tilde{y}_i$ are passed to the classifier. The ℓ_1 classifier first finds the sparse coefficient vector x_i. Then the vectors of different gait cycles are fused based on a novel *sparse fusion* model, and the fused sparse vector is used to calculate the residuals. Finally, the identity is obtained by finding the minimal residual.

In the following sections, we detail the design of signal pre-processing, offline dictionary training, and classification in turn.

B. Signal Pre-processing

1) Gait Cycle Segmentation: In order to recognize a gait signal, it is essential that we separate the time series of walking periods into segments, such that each segment contains a complete gait cycle. The gait cycle can be obtained by combining two successive step cycles together as technically the gait cycle is across a *stride* (two steps). As mentioned in [28], typical step frequencies are around 1-2Hz, we apply a band-pass Butterworth filter [29] on the sampled data to eliminate out-band interference. The lower and upper cutoff frequency is set as 1Hz and 2Hz separately (filter order is 4). After filtering, the step cycles are separated by finding peaks associated with the heel strike as shown in Figure 6. Thereafter, the gait cycle is obtained by combining two consecutive step cycles together.

After gait cycle extraction, the output voltage data are segmented into short gait cycles based on the peak detection. Figure 7 presents the distribution of cycle duration (i.e. time length of stride) for 20 healthy subjects walking at their normal speed. We can see that most of the gait cycle ranges between 0.8-1.3s (80-130 samples at 100Hz sampling rate). This results in turn can be used to omit unusual gait cycles and exclude the cycles not produced by walking, i.e., the cycles which last less than 0.8s and exceed 1.3s are dropped.

2) Linear Interpolation: Detected cycles are normalized to equal length by linear interpolation because SRC requires vectors of equal length as input. As mentioned above, normal gait duration lies between 80 and 130 samples, we apply linear interpolation on the samples to ensure that they achieve the same length of 130 samples.

C. Offline Training

The training data are also passed to gait cycle segmentation and linear interpolation to obtain gait cycles with same length. In addition, we delete unusual cycles and optimize projection matrix to further improve recognition accuracy.

1) Deletion of Unusual Cycles: Unusual cycles caused by occasional abnormalities like temporary walking pauses or

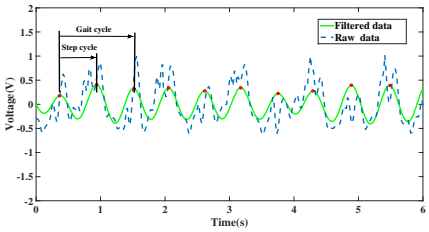

Fig. 6: The time series of harvested energy: raw data (blue dash line), filtered data (green solid line).

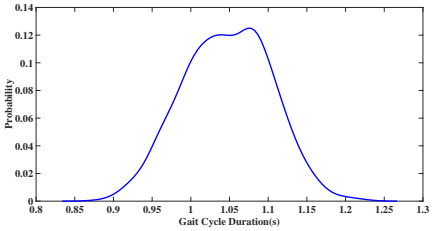

Fig. 7: Distribution of cycle duration

turning contains much noise that will deteriorate the recognition accuracy. Apart from deleting unusual cycles using cycle durations, the detected cycles are also passed to a function which further deletes unusual cycles. This function uses Dynamic Time Warping (DTW) distance scores to remove outliers from a set of cycles. Specifically, we first compute the DTW distance between the detected cycle and typical cycle. Thereafter, we delete unusual cycles by a simple threshold method, i.e., if the DTW distance of detected cycle and typical cycle is higher than a predefined value (12 in the proposed system), the detected cycle will be dropped. The typical cycle is the one which is assumed to represent the subject's gait signal. This is obtained by computing the the average of all cycles in the training data.

2) Projection Optimization: After unusual cycles removal, the remaining gait cycles obtained from training data are used to form the final training dictionary A. Motivated by a recent work [27], we apply the projection matrix optimization method proposed in [27] to reduce the dimensionality of SRC while retaining the high classification accuracy. The projection matrix R_{opt} is learned from dictionary A based on Tabu search [30]. We refer the reader to [30] for more details.

D. MSSRC

SRC aims to solve the classification problem of one test vector, however, the evaluation results in Section VI-C show that the recognition accuracy of using one gait cycle can achieve 86% (PEH dataset) and 75% (EEH dataset) only. To overcome this limitation, we propose a novel *sparse fusion* model which fuses the sparse coefficients vectors from multiple consecutive gait cycles to further improve recognition accuracy.

The key assumption behind the proposed method is that gait cycles obtained from consecutive gait cycles tend to have a high agreement on the sparse representations because each of the gait cycles from the same person should be linearly represented by the same class in the dictionary. Suppose we have acquired a set of M gait cycles from the test signal. Following the single test vector approach described in Section II, we can obtain a set of estimated coefficients vectors $\hat{X} = \{\hat{x}_1, \hat{x}_2, ..., \hat{x}_M\}$ by solving the ℓ_1 optimization problem for each gait cycle. Theoretically, a precise sparse representation will only contain the non-zero entries at the locations related to the specific class. However, noise exists in the empirical estimations. Therefore, the estimated coefficients vector of the m-th test gait cycle can be expressed as:

$$\hat{x}_m = x + \epsilon_m \tag{1}$$

where x is the theoretical sparse representation of the test vector and ϵ_m is used to account for noise. The test vector could be misclassified due to low Signal to Noise Ratio (SNR). To enhance the SNR of the classification system, we propose a new sparse representation model by exploiting the information from multiple gait cycles. The new sparse representation model can be expressed as:

$$\hat{x}_{sum} = \sum_{m=1}^{M} \alpha_m \hat{x}_m \tag{2}$$

where α_m is the weight assigned to $\hat{x}_m$ based on the *Sparsity Concentration Index* (SCI) defined in [31]:

$$SCI(\hat{x}_m) = \frac{K \cdot max_j \|\delta_j(\hat{x}_m)\|_1 / \|\hat{x}_m\|_1 - 1}{K - 1} \in [0, 1] \tag{3}$$

the SCI measures how concentrated the coefficients are in the dictionary. $SCI(\hat{x}_m) = 1$, if the test vector can be strictly linearly represented using training vectors from only one class; and $SCI(\hat{x}_m) = 0$, if the coefficients are spread evenly over all classes. The weight of $\hat{x}_m$ is obtained by normalizing the SCIs among the obtained M gait cycles:

$$\alpha_m = SCI(\hat{x}_m) / \sum_{n=1}^{M} SCI(\hat{x}_n) \tag{4}$$

With the knowledge of $\hat{x}_{sum}$, the compressed residual of each class is computed as:

$$r_i(y_{sum}) = \|R_{opt} y_{sum} - R_{opt} A \delta_i(\hat{x}_{sum})\|_2 \tag{5}$$

where $y_{sum} = \sum_{m=1}^{M} \alpha_m y_m$ is the weighted summation of all the test vectors. Following the same approach in [31], [27], the final classification result is obtained by finding the minimal residual.

To identify whether the walker is the genuine user or imposter, we adapt the same principle in [27] by using confidence level defined as:

$$confidence = \left(\frac{1}{K} \sum_{i=1}^{K} r_i - \min_{i=1,...,K} r_i \right) / \frac{1}{K} \sum_{i=1}^{K} r_i \tag{6}$$

The confidence level is in the range of $[0, 1]$ and the verification decision can be made by:

$$confidence \begin{cases} \geq C & \text{genuine user} \\ < C & \text{imposter} \end{cases}$$

where C is a threshold we set empirically. An appropriate threshold can be chosen by data-driven approach to make the recognition system robust to imposters.

V. Hardware Platform and Data Collection

A. Proof-of-concept Prototype

PEH data logger. To this end, we built a data logger to collect PEH voltage signals. The data logger includes a vibration energy harvesting product from the MIDÈ Technology called Volture, which implements the transducer to provide AC voltage as its output. Our hardware also includes a 3-axis accelerometer to record the acceleration signals, simultaneously with the voltage signal. An Arduino Uno has been used as a microcontroller device for sampling the data from the Volture. A sampling rate of 100Hz has been used for data collection. The sampled data has been saved on an 8GB microSD card which has been equipped to the Arduino using microSD shield. A nine volts battery has been used to power the Arduino. To control the data collection, our data logger also includes two switches, one is an on/off switch and the other to control the start and stop of data logging. The Arduino measures voltage between 0 and 5 volts and provides 10 bits of resolution (i.e., 1024 different values). Therefore, we calculated the corresponding output voltage from the measurements using the following formula $V = \frac{5*measurement}{1023}$. The hardware platform and the internal appearance of the data logger are shown in Figure 8.

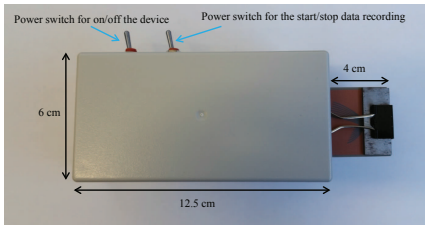

(a)

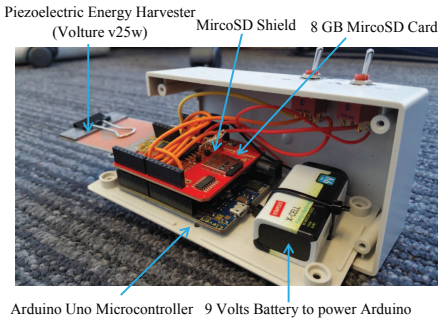

(b)

Fig. 8: PEH data logger: (a) the external appearance and (b) the internal details.

EEH data logger. We also built an EEH data logger to collect voltage signals generated from an EEH device. The data logger contains a harvesting circuit, through which energy is generated by moving a magnet through an inductor. A Tmote sky board has been used as a microcontroller device for sampling the data from the inductor. A sampling rate of 100Hz has been used for data collection. The sampled data has been saved in the 48K Flash of the MSP430 microcontroller. Two AA batteries has been used to power the Tmote sky board. We use a button to control the data collection.

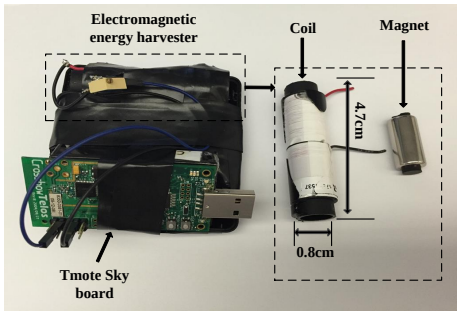

Fig. 9: EEH data logger

(a) Indoor experiment

(b) Outdoor experiment

(c) Holding PEH device

(d) Holding EEH device

Fig. 10: The illustration of data collection.

B. Data Collection

The dataset used to evaluate the performance of the proposed system consists of 20 healthy subjects (14 males and 6 females)[5]. During the data collection phase, the participants were asked to hold the data logger in their preferred hand and walk at their normal speed (0.7-1.1m/s). The data collection is performed in several environments (indoor and outdoor) in order to capture the influence of different terrains. An illustration of indoor environment and outdoor environment is shown in Fig 10(a) and Fig 10(b). The terrain of the chosen outdoor environment varies including plain, grass and asphalt. Each volunteer participated in two data collection sessions that was separated by one week. During each session, the participants were asked to hold the device (see Fig 10(c) and Fig 10(d)) and walked along the specific route shown in Figure 10(a) and Figure 10(b) for approximately 5 minutes. Based on the above description, the gait dataset is close to a realistic environment as it includes the natural gait changes over time and different environments (indoor and outdoor). In total, we have collected over 300 seconds of samples for each subject from the EH devices as well as the accelerometer. We collect two voltage datasets by using the PEH and EEH devices, respectively, and perform gait cycle segmentation and unusual gait cycle deletion on both of the datasets, and finally we extract 200 gait cycles from each subject for evaluation.

[5]Ethical approval for carrying out this experiment has been granted by the corresponding organization (Approval Number HC15304 and HC15888)

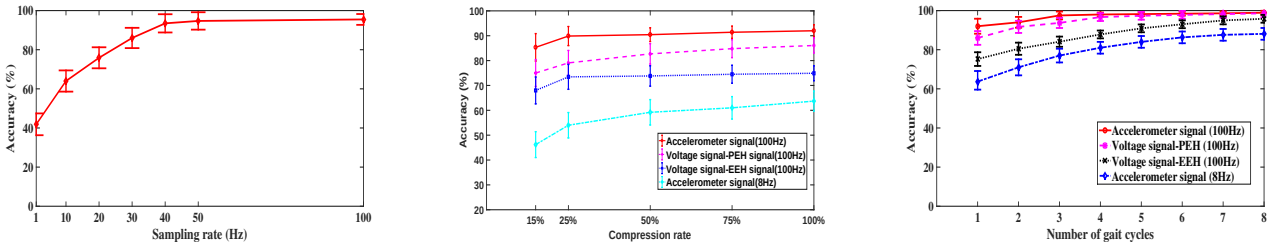

(a) (b) (c)

Fig. 11: (a) Recognition accuracy vs sampling rate. (b) recognition accuracy under different compression rate when k=1. (c) recognition accuracy under different number of gait cycles when $= 75\%$.

VI. Evaluation

A. Goals, Metrics and Methodology

In this section, we evaluate the performance of the proposed system based on the collected dataset. The goals of the evaluation are threefold: 1) investigate the relation between recognition accuracy and sampling rate of accelerometer data; 2) compare the recognition accuracy of KEH-Gait with that of using accelerometer data; 3) compare the proposed classification method in KEH-Gait with several state-of-the-art classification algorithms.

In this paper, we focus on the following three evaluation metrics:

- **Recognition accuracy**: it represents the percentage of correct classifications which is simply the number of true classifications over the total number of tests.
- **False positive rate (FPR)**: probability that the authentication system incorrectly accepts the access request by an imposter.
- **False negative rate (FNR)**: probability that the authentication system incorrectly rejects the access requests from the genuine users.

The recognition accuracy of KEH-Gait is obtained by using output voltage in one gait cycle as a test vector. For fair comparison, we perform the same signal processing and classification method on acceleration data. The only difference is the test vector is obtained by concatenating acceleration data along three axes in one gait cycle together. In the evaluation, we compare MSSRC with Support Vector Machine (SVM), K-Nearest Neighbor (KNN), and Naive Bayes (NB). The intuition of we use SRC is that it has shown better performance than traditional classification methods (e.g., SVM and KNN) in recognition tasks of sensor areas such as face recognition [27], [32] and voice recognition [33]. SRC is known to be robust to noise because of its use of ℓ_1 optimization [27]. Thus, we use SRC in KEH-Gait and improve its performance by exploring the sparsity of testing vectors as discussed in Section IV-D. The parameters in SVM, KNN and NB are well tuned to give highest accuracy. For KNN classifier we set the number of nearest neighbors as 10. For SVM classifier, we choose linear kernel function, and the soft margin constant is set 10. We choose normal Gaussian distribution for NB. For each classifier, we perform 10-fold cross-validation on the collected dataset. Specifically, we randomly split the dataset into 10 folds with equal size. Then, each fold is retained as the validation data for testing the classifier, and the remaining 9 folds are used as training data. The cross-validation process is then repeated 10 times, with each of the 10 folds used exactly once as the testing data. In the evaluation, we let k denote the number of gait cycles fused to perform classification and σ denote the compression rate. The compression rate means the number of projections/features over the dimension of original testing vector. We plot the results of the average values and 95% confidence level of the recognition accuracy obtained from 10 folds cross-validation.

B. Recognition Accuracy v.s. Sampling Rate

In the first experiment, we evaluate the impact of sampling rate on the gait recognition accuracy of acceleration data. The goal is to investigate the relation between recognition accuracy and the consumed power of accelerometer, as the power consumption is directly related to the sampling rate. We use MSSRC as the classifier and calculate the recognition accuracy at different sampling rates by subsampling the acceleration data from 100Hz to 1Hz. As shown in Figure 11(a), the recognition accuracy increases with growing sampling rate. This is intuitive as the more measurements are sampled, the more information is available, and thus, enabling more accurate classification. However, the improvement diminishes after the sampling rate is greater than 40Hz. The results indicate that to achieve high recognition accuracy, a sampling rate of at least 40Hz is required. In the rest of the evaluation, we limit our discussion on sampling at 40Hz.

As we will discuss in Section VII-B1, the power consumption of accelerometer-based system will increase significantly with the rising sampling frequency. Based on our measurement results, the accelerometer-based system consumes approximately $300\mu W$ with 40Hz to achieve accurate recognition. However, this consumption requirement is far beyond the actual power generated by the energy harvester (neither PEH, nor EEH). According to a recent theoretical study of energy harvesting from human activity [11], assuming 100% conversion efficiency, the power can be harvested from walking is only $155\mu W$. Unfortunately, in practical, according to our measurement results, the average power produced from walking is $19.17\mu W$ using EEH, and approximately $1\mu W$ using PEH which is not tuned specifically for human activity energy harvesting. In this case, due to the limited amount of power that is available to power the system, its sampling frequency will decrease below 40Hz. As a result, the recognition accuracy

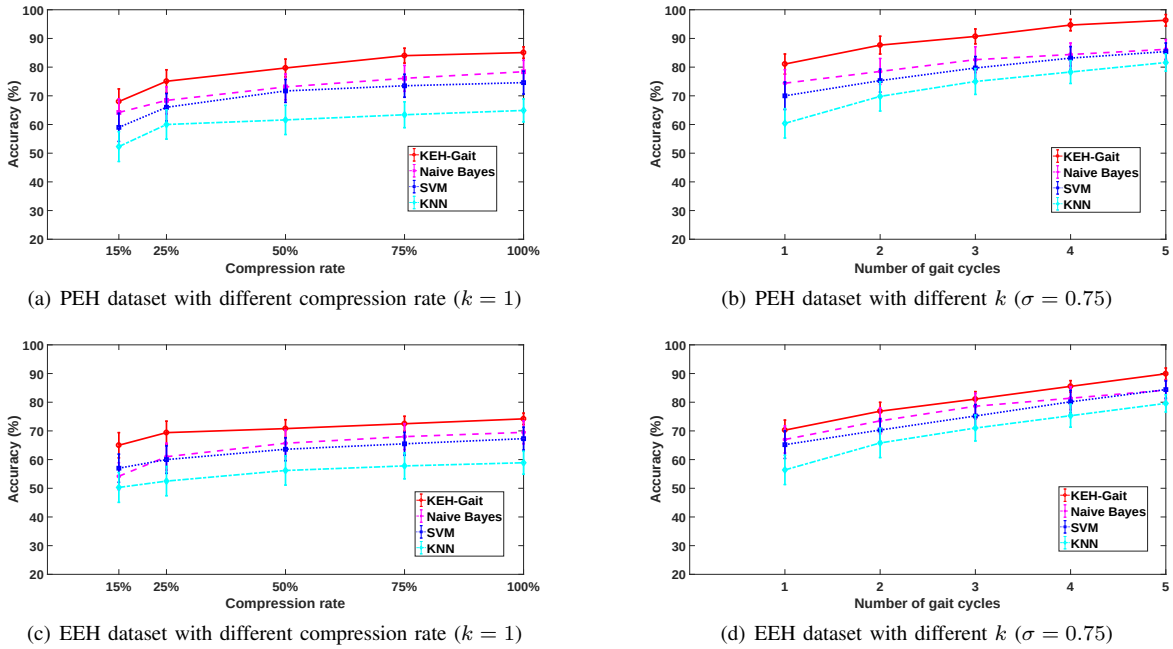

(a) PEH dataset with different compression rate ($k = 1$)

(b) PEH dataset with different k ($\sigma = 0.75$)

(c) EEH dataset with different compression rate ($k = 1$)

(d) EEH dataset with different k ($\sigma = 0.75$)

Fig. 12: Comparison with other classification methods on two datasets (sample rate 40Hz).

will dramatically decrease accordingly. The results highlight the necessity of using kinetic voltage signal to achieve gait recognition directly, instead of using the accelerometer signal. In the next subsection, we will show that the recognition accuracy of using kinetic voltage signal is comparable to that of using accelerometer data.

C. KEH-Gait v.s. Accelerometer-based System

In this section, we investigate whether KEH-Gait can achieve comparable accuracy compared to accelerometer signal. In case of using accelerometer signal, we calculate the recognition accuracy at two different sampling rates: 1) raw sampling rate (100 Hz) of the data logger; and 2) the highest achievable sampling rate of the accelerometer if it is powered by the energy harvester. From our dataset, the energy harvester can generate 19.17 μW on average from walking. Thus, according to the handbook of MPU9250 which is used in our prototypes, it can sample at most 8Hz if it is powered by the energy harvester.

In this experiment, we set $k = 1$ and calculate the recognition accuracy by varying compression rate σ from 15% to 100%, and the results are plotted in Figure 11(b). We can see that the recognition accuracy of using voltage signal is significantly higher than that of using accelerometer at sampling rate of 8Hz. This suggests that the harvested power cannot support the accelerometer to sample at a high frequency which leads to low recognition accuracy; instead, using the voltage signal itself is able to achieve higher recognition accuracy. However, the recognition accuracy of using voltage signal is still approximately 6% (PEH) and 17% (EEH) below than that of using raw accelerometer signal when $\sigma = 100\%$.

We now demonstrate that the recognition accuracy of using harvested power signal can be improved significantly by the proposed MSSRC, and it reaches a comparable recognition accuracy compared to using the raw accelerometer signal. In this experiment, we set $\sigma = 75\%$ as the accuracy improvement diminishes when the number of projections/features increased to 200 as shown in Figure 11(b). Then we calculate the recognition accuracy of KEH-Gait using accelerometer signal and voltage signal, while increasing k from 1 to 8. From the results in Figure 11(c), we notice that the recognition accuracy is improved significantly when more gait cycles are fused together. The result is intuitive as more information can be obtained to identify the subject by using more gait cycles. We also find that by using voltage signal of PEH, we can achieve a comparable accuracy compared to using raw accelerometer signal when $k = 8$, and the recognition accuracy of EEH is slightly lower (3%) than using raw accelerometer signal. In the real application, k can be tuned by the healthcare company to satisfy their own needs. For example, a larger k makes the system more secure to the imposters while it sacrifices user experience because it will take more time to collect required steps.

D. Comparison with Other Classification Methods

We now evaluate whether MSSRC outperforms other state-of-the-art classification algorithms. Specifically, we compare MSSRC with SVM, KNN, and NB. We perform comparison on two datasets separately.

Performance on PEH dataset. We follow the same experimental procedure in Section VI-C to evaluate the recognition accuracy of different methods under different d (number of projections/features). From Figure 12(a), we find that KEH-Gait improves recognition accuracy by up to 7% compared to the second best classification method (i.e., NB). We further evaluate the recognition accuracy of SVM, KNN and NB by combining several gait cycles together. As KEH-Gait utilizes multiple gait cycles to find the final classification result, we apply the majority voting scheme to achieve a fair comparison. Specifically, we first obtain the identity of each gait cycle by

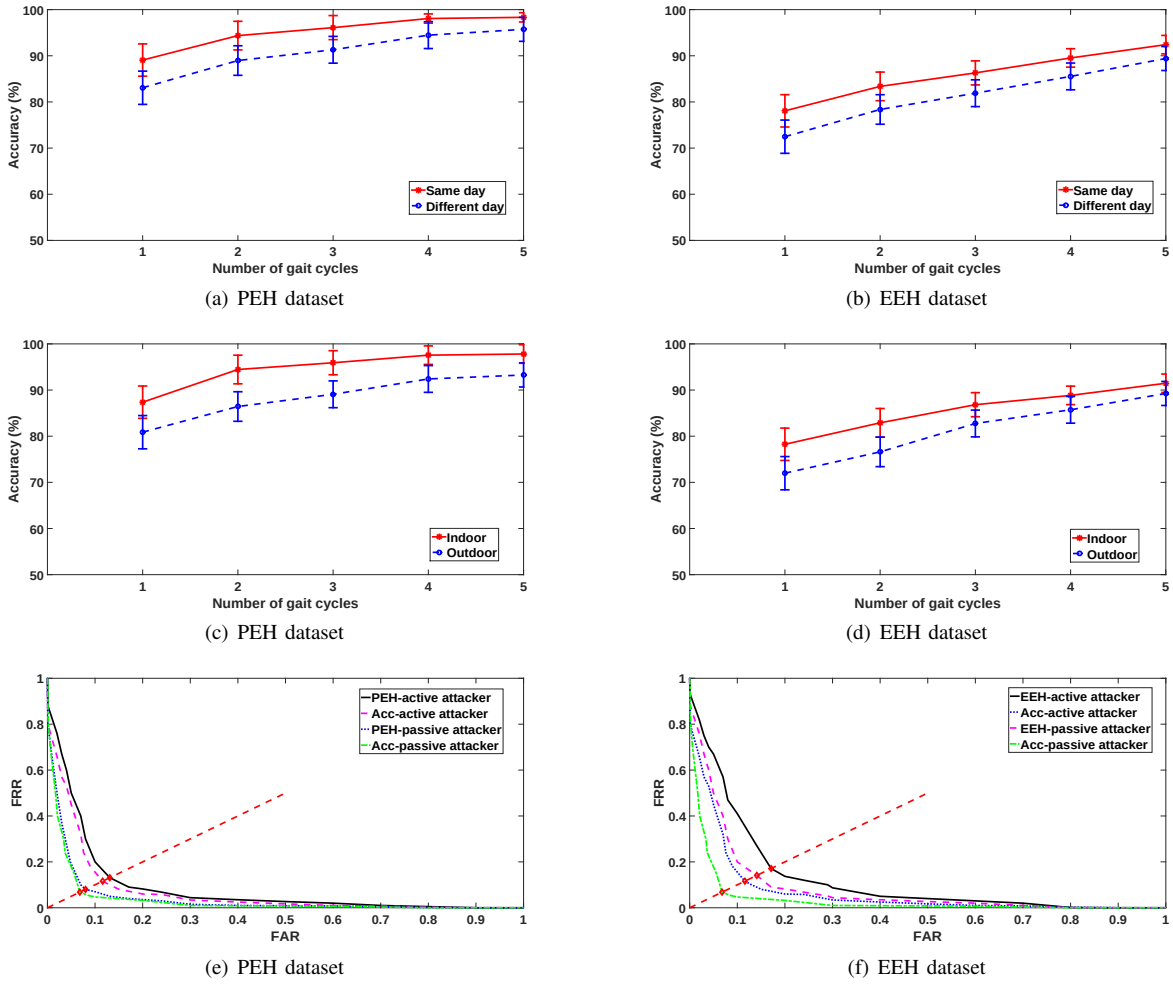

(a) PEH dataset (b) EEH dataset

(c) PEH dataset (d) EEH dataset

(e) PEH dataset (f) EEH dataset

Fig. 13: Evaluation results: (a)-(d) robustness to gait variations. (e)-(f) robustness against attackers.

using SVM, KNN and NB, then we apply majority voting scheme to combine the results together, the subject with the highest voting is declared to be the recognized person. Again, we set $\sigma = 75\%$ and calculate the recognition accuracy of different methods by varying k from 1 to 5 (number of gait cycles). From the results in Figure 12(b), we find that KEH-Gait consistently achieves the best performance and is up to 10% more accurate than the second best approach (i.e., NB). The improvement of MSSRC over other methods is because MSSRC exploits the sparsity information from multiple gait cycles.

Performance on EEH dataset. We perform the same steps as above on EEH dataset and plot the results in Figure 12(c) and Figure 12(d). The results show that KEH-Gait is 6% better than NB when $\sigma = 75\%$, $k = 1$, and 4% better than NB when $\sigma = 75\%$, $k = 5$. We also find that the overall performance on EEH dataset is lower than that on PEH dataset. We believe the drop on recognition accuracy is caused by the fact that the magnet is not sensitive to slight vibrations and motions.

The results in this section suggest that the proposed MSSRC in KEH-Gait can improve recognition accuracy significantly by fusing several steps together and outperform several state-of-the-art classification algorithms. Another straightforward method to apply SRC on multiple steps is to first apply SRC on each step and then obtain the final results by majority voting scheme. We found that MSSRC is approximately $3\% - 7\%$ more accurate than direct majority voting on our dataset since it exploits the sparsity information of multiple measurements. Due to limited space, we do not plot the results of direct major voting in this paper.

E. Robustness to Gait Variations

To evaluate the robustness of KEH-Gait to gait variations, we conduct the following two experiments: different day evaluation and different environment evaluation. In this experiment, same day evaluation means the training set and test set are chosen from the sessions of the same day while different days evaluation chooses the sessions from two different days separated by 1 week. Similarly, in different environment evaluations, indoor evaluation means the training set and test set are chosen from indoor environment while outdoor evaluation chooses training data and test data from outdoor environment. We conduct this evaluation on PEH dataset and EEH dataset respectively. As the results in Figure 13(a) and Figure 13(b), the accuracy of different day is lower than the same day evaluation as the different days evaluation tends to produce more changes to gait. However, KEH-Gait can still achieve the accuracy of 95% and 89% on the two dataset respectively

when more than 5 steps are used. This observation holds in the different environment evaluation. From Figure 13(c) and Figure 13(d), we can see outdoor environment achieves lower accuracy than indoor environment because it includes several different terrains such as grass path and asphalt road. Gait changes can be caused many other factors such as speed and shoes etc.. We further discuss the influence of these factors in Section VIII-B.

F. Robustness Against Attackers

As mentioned in Section III, we assume the presence of a passive adversary and an active attacker during an authentication session. We evaluate the robustness of the proposed system against the eavesdropper and active attacker by conducting the following two imposter attempt experiments.

- A passive imposter attempt is an attempt when an imposter performs authentication using his own walking pattern. This attack happens when the genuine user passes his device to another person to spoof the healthcare system.
- An active imposter attempt means the imposter mimics the gait of the genuine user with the aim to spoof the healthcare system. This attack happens when the several users collude to fool the healthcare system.

The first experiment is conducted to evaluate the robustness to a passive imposter. In this experiment, we use the raw voltage signal from other subjects as passive imposter attempts. We then repeat this experiment by testing all the steps of the 20 subjects in the dataset. To evaluate the robustness against the second imposter attack scenario, we group the 20 subjects into 10 pairs. Each subject was told to mimic his/her partner's walking style and try to imitate him or her. Firstly, one participant of the pair acted as an imposter, the other one as a genuine user, and then the roles were exchanged. The genders of the imposter and the user were the same. They observed the walking style of the target visually, which can be easily done in a real-life situation as gait cannot be hidden. Every attacker made 5 active imposter attempts. The authentication accuracy is evaluated by FPR and FNR. In general, FPR relates to the security of the system, while FNR to the usability. An interesting point in the Decision Error Trade-off (DET) curve is the Equal Error Rate (EER) where FPR=FNR. For instance, an EER of 5% means that out of 100 genuine trials 5 is incorrectly rejected, and out of 100 imposter trials 5 are wrongfully accepted. We set $k = 5$ and vary the confidence threshold C to plot DET curve in Figure 13.

The results on two dataasets are plotted in Figure 13(e) and Figure 13(f) respectively. The red dash line stands for the possible points where FPR is equal to FNR. The crossover (marked as a diamond) of the red dash line and FPR-FNR curve stands for the location of the EER. We notice that EER of KEH-Gait is 8.4% and 14.1% on the two datasets respectively, which means out of 100 passive imposter trials 8 are wrongfully accepted by using PEH and 14 are wrongfully accepted by using EEH. We also find that an imposter does benefit from mimicking the genuine user's walking style. The EER increases to 13.3% and 17.1% on the two datasets respectively. For the accelerometer-based system, the EER of a passive attacker and an active attacker are 6.8% and 11.6%, respectively. The results indicate that the PEH-based system can achieve comparable EER compared to the accelerometer-based system. The individual nature of walking gait provides our scheme security against impersonation attackers and the evaluation results are encouraging. The false negatives occur when the gait patterns of the imposter and user are close. This problem could be dealt with by using two factor authentication.

VII. Energy Consumption Profile

Battery lifetime is widely regarded as the major barrier of achieving long term human-centric sensing. Reducing system energy consumption has attracted tremendous research efforts in both academics and industries. In this section, we will conduct an extensive energy consumption profiling of state-of-the-art wearable systems.

The energy consumption of our system consists of three parts: sensor sampling, memory reading/writing, and data transmission. We find that memory reading/writing consumes significant less energy compared to the other two parts. A recent study [34] also investigates the energy consumption of different Random Access Memory (RAM) technologies, and their findings support our measurement results. According to their measurement, it only consumes 203pJ to write to (or read from) Static Random Access Memory (SRAM) which is used in SensorTag. That means if we collect 5s gait data at 40Hz, it only takes $5 \times 40 \times 203$ =40.6nJ to read or write data. Compared to the energy consumption of other parts, the energy consumed by SRAM is negligible. Therefore, we only consider the energy consumption of sensor sampling and data transmission in our evaluation.

A. Measurement Setup

The Texas Instrument SensorTag is selected as the target device, which is embedded with the ultra-low power ARM Cortex-M3 MCU that is widely used by today's mainstream wearable devices such as FitBit. The SensorTag is running with the Contiki 3.0 operating system. The experiment setup for the power measurement is shown in Figure 14(a). In order to capture both the average current and the time requirement for each sampling event, the Agilent DSO3202A oscilloscope is used. As shown in the figure, we connect the SensorTag with a 10Ω resistor in series and power it using a 3V coin battery. The oscilloscope probe is then connected across the resistor to measure the current going through.

B. Energy Consumption of Sensor Sampling

1) Power Consumption of Sampling Accelerometer: The SensorTag includes 9-axis digital MPU9250 motion sensor combining gyroscope, digital compass, and accelerometer. During the power measurements, we only enable the 3-axis accelerometer and leave all the other sensors turned off. The acceleration signal is sampled using the Inter-Integrated Circuit (I^2C) bus with a sampling frequency of 25Hz. Note that, it is also possible for the wearable devices to use analog accelerometers, which can be sampled through analog-to-digital converter (ADC) instead of I^2C bus. Sampling analog accelerometers could avoid power consumption and additional time requirement due to the I^2C bus, but at the expense of some processing costs in analog to digital converting. While it is not immediately obvious whether analog accelerometer

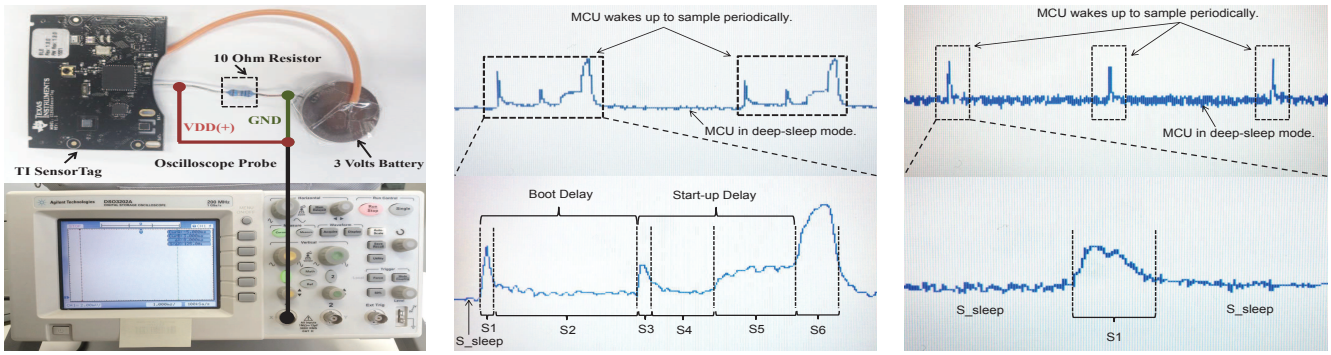

(a) Experimental setup for power measurement. (b) Profiling of accelerometer sampling. (c) Profiling of voltage sampling.

Fig. 14: Measurement setup and results.

sampling would be less or more power consuming relative to the digital counterpart, a detailed measurement study [35] indicates that digital accelerometer is more power efficient than the comparable analog ones from the same manufacturers.

TABLE I: States of accelerometer sampling, which takes 17.2ms in total and consumes 322μW.

State	Time (ms)	Power (uW)
S1	0.6	768
S2	7.2	72
S3	0.6	480
S4	3.2	72
S5	4	480
S6	1.6	1440
S_sleep	null	6

Figure 14(b) shows the details of accelerometer sampling energy profile. As shown, each accelerometer sampling event can be divided into six states. At the beginning of each event, the MCU is waked up by the software interrupt from the power-saving deep-sleep mode (S_sleep), and it boots the accelerometer (S1) before going back to sleep. During S2, the accelerometer starts to power up while the MCU is in sleep mode. Then, after one software clock tick (7.8 ms in Contiki OS), the MCU wakes up again by the interrupt to initialize the accelerometer (S3) and then goes back to sleep. The accelerometer starts initializing in S4 and turning on in S5. Finally, MCU wakes up in S6 to sample the acceleration signal and then goes back to deep-sleep again. The average power consumption and time requirement for each state are shown in Table I.

2) Power Consumption of Sampling KEH: In this subsection, we investigate the power consumption in sampling the voltage signal of the power source. During the measurement, MCU is programmed to periodically sample the voltage of the lithium coin battery with 25Hz sampling rate. The MCU reads voltage signal through ADC. Figure 14(c) shows the details of voltage sampling. Similar to the accelerometer, the MCU goes back to deep-sleep mode after each sampling event. However, sampling the voltage takes only 0.6ms, which is much shorter than the 17.2ms required by the accelerometer sampling. This is because the MCU can read the voltage signal directly without having to prepare the hardware to be powered-up, and the voltage signal to be prepared by the power source. The details of power consumption and time duration for voltage sampling event are shown in Table II.

TABLE II: States of voltage sampling.

State	Time (ms)	Power (μW)
S1	0.6	480
S_sleep	null	6

3) Energy Consumption Comparison: We now compare the energy consumption of sampling accelerometer and KEH. In general, for the duty-cycled gait-recognition system, the average power consumption in data sampling, P_{sense}, can be obtained by the following equation:

$$P_{sense} = \begin{cases} \frac{T_S \times n}{1000} P_{sample} + (1 - \frac{T_S \times n}{1000}) P_{sleep} & \text{if } 0 \leq n \leq \frac{1000}{T_S}, \\ P_{sample} & \text{if } \frac{1000}{T_S} < n. \end{cases} \quad (7)$$

where, P_{sample} is the average power consumption in the sampling event (either sampling acceleration or KEH signal), and P_{sleep} is the average power consumption when the MCU is in deep-sleep mode (with all the other system components power-off). n is the sampling frequency, and T_S is the duration of time (in milli-second) spent in a single sampling event. Based on the measurement results given in Table I and Table II, we can obtain the average power consumption for the accelerometer sampling event equals to 322μW with a time requirement of 17.2ms, and 480μW with a duration of 0.6ms for the KEH sampling event. Then, based on Equation 7, we get the power consumption in data sampling for both accelerometer-based and KEH-based gait-recognition systems with different sampling frequencies. The results are compared in Figure 15. It is clear to see that the proposed KEH-Gait achieves significant power saving in data sampling, comparing with the conventional accelerometer-based gait-recognition system. More specifically, given the analysis shown in Figure 11(a), a sampling rate higher than 40Hz is needed to achieve high recognition accuracy. With a 40Hz sampling frequency, in case of data sampling, KEH-Gait consumes 17.38μW, while the power consumption of accelerometer-based system is 230.74μW.

As can be seen from Figure 11(c), to achieve the same recognition accuracy, it needs to collect 3 gait cycles for the accelerometer-based system and 5 gait cycles for the KEH-based system. If we assume one gait cycle takes 1s (the average time of one gait cycle is between 0.8s-1.2s), this results in 86.9μJ and 692.22μJ energy consumption in data sampling

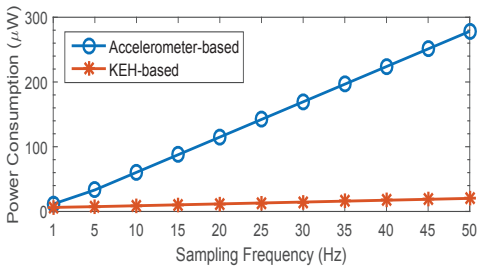

Fig. 15: Power consumption comparison.

for KEH-Gait and accelerometer-based system, respectively.

C. Energy Consumption of Data Transmission

Next, we evaluate the energy consumption of transmitting acceleration and KEH voltage data via Bluetooth. We conduct power measurement of the Bluetooth Low Energy (BLE) beacon using the embedded CC2650 wireless MCU in the SensorTag. With the 40Hz sampling rate and 75% compression rate, KEH-Gait generates 200 voltage samples every five seconds. This results in 300 bytes data to be transmitted in total (2 bytes for each of the 12-bits ADC voltage reading). This consumes an average power of 2.72mW with a transmission time of 52ms, which results in 106.08μJ of energy consumption. On the other hand, as 3-axis acceleration data is collected for 3s, it results in 540 bytes of data and the energy consumption of transmitting those data is 190.94μJ.

D. Total Energy Saving Analysis

After obtaining the energy consumption of sensor sampling and data transmission, we investigate the potential of KEH-Gait for energy saving. Based on the measured results, the energy consumption of KEH-Gait to complete one authentication is approximately 192.98μJ, which has reduced the energy consumption of the accelerometer-based system (883.16μJ) by 78.15%.

A recent study [35] tested the power consumption of six most commonly available accelerometers, and they found that when the sampling rate is 50 Hz, the mean power consumption of these accelerometers is 1542μW, and the minimum power consumption is 518μW. These accelerometers consume more power than the one used in our experiments. These results indicate that KEH-Gait is still superior to most commonly used accelerometers in terms of energy savings. On the other hand, the power consumption of accelerometers can be further reduced by use of data buffers. For example, ADXL345 can store 32 samples automatically without waking up the CPU. However, similar optimisation technique can also be integrated in the KEH-based system to reduce the system level energy consumption. In this way, the energy consumption of both accelerometer-based system and KEH-based system will be reduced. We defer the design optimization of buffer-enabled KEH-Gait to our future work.

VIII. Discussion

A. PEH v.s. EEH

In this study, we analyze the feasibility of using power signal generated from energy harvester for gait recognition purpose. Specifically, we focus on two types of kinetic energy harvester: PEH and EEH. Our study demonstrates the harvested power signal caused by human gait motions can be used to identify different individuals. Table III summarizes a comparison between the PEH and EEH devices we used in this paper.

TABLE III: Comparison between PEH and EEH used.

	Size (cm × cm × cm)	Weight (grams)	Accuracy (%)	Power (uW)	Cost (USD)
PEH	4.6 × 3.3 × 0.1	23.5	86.1	1	157
EEH	4.7 × 0.8 × 0.8	65	75.2	19.17	37.5

The first observation we can have is that the PEH we used achieves higher recognition accuracy and generates more energy than EEH when the user is holding the device in the hand and walk normally. The results can be explained by our observation that the EEH contains a heavy magnet which is not sensitive to weak vibrations and motions (compared in Figure 4(c) and 4(e)). This results in a roughly 10% difference in the recognition accuracy.

In addition to the system performance, another important characteristic in designing a wearable device is the form factor and weight. In case of the PEH device, we built it upon the Volture V25W PEH energy harvester with a 4.6cm × 3.3cm × 0.1cm form factor. And it can be further reduced to 2.2cm × 0.4cm × 0.1cm by exploiting smaller harvester produces such as the PPA-1022. On the other hand, the EEH device requires large mass displacement to ensure the free movement of magnet which makes it difficult to reduce the form factor. Moreover, in order to generate more power from the PEH device, a 20 grams tip mass is attached to the PEH device and results in an overall weight of 23.5 grams. Fortunately, with current advancement in PEH design, the overall weight of the PEH can be reduced to less than 10 grams without significantly sacrificing the output power. In comparison, the EEH device includes a heavy magnet and results in a weight approximately 65 grams in total. Given the above facts, we believe that PEH is more convenient to be embedded in future wearable devices that have strict constraint in size and weight.

Finally, the price of the PEH we used in our prototype is approximately 157USD (Volture V25W), while the cost of the EEH we used is 37.5USD. Although both of the prices can be largely reduced with a larger quantity of purchase, the cost of building the PEH device is higher than that of the EEH device.

B. Factors Affecting Gait Recognition

Many factors exist that may impact the accuracy of a gait-based recognition system, such as shoe, clothes, walking speed and terrain. Previous studies have shown that the accuracy will decrease when the test and training samples of the person's walking are obtained using different shoe types and clothes [36]. Indeed, as shown in Section VI-E, the accuracy of KEH-Gait decreases when session 1 is used for training and session 2 is used for testing. The dataset used in the experiment is challenging as it includes the natural gait changes over time (two sessions separated by 1 week), as well as gait variations due to changing in clothes, terrain and shoes. However, KEH-Gait can still achieve the accuracy of 95% and 89% on the two dataset respectively by the proposed MSSRC, which in turn demonstrate the robustness of KEH-Gait to gait variations.

The focus of our study is to demonstrate the feasibility of gait recognition using KEH and improve its performance. Due to space limitation, we defer the analysis of different factors to our future work. In fact, there has been several attempts to study the relationship between recognition performance and different factors [36], [37]. For example, in terms of walking speed, Muhammad and Claudia [37] found that normal walk has best results and fast walk is a bit better than slow walk. As for different types of terrains, they reported that gravel walk has better results than grass and inclined walk. We encourage the reader to refer to [36], [38], [37] for more details.

IX. Related work

Gait Recognition: Gait recognition has been well studied in the literature. From the way how gait is collected, gait recognition can be categorized into three groups: vision based, floor sensor based, and wearable sensor based. In vision based gait recognition system, gait is captured from a remote distance using video-camera. Then, video/image processing techniques are employed to extract gait features for further recognition. A large portion in the literature belong to this category [39], [40], [41], [42]. In floor sensor based gait recognition, sensors (e.g., force plates), which are usually installed under the floor, are used for capturing gait features, such as ground reaction force (GRF) [43] or heel-to-toe ratio [44].

Compared with vision-based and other non-accelerometer based gait measurements, acceleration can reflect the dynamics of gait more directly and faithfully. For instance, accelerometer based gait recognition do not suffer from the existing problems for vision-based methods, like occlusions, clutter, and viewpoint changes. Existing works of wearable sensor based gait recognition are mainly based on the use of body-worn accelerometers. The first work of accelerometer based gait recognition is proposed by Ailisto et al. [8] and further developed by Gafurov et al. [45]. In the initial stages, dedicated accelerometers were used and worn on different body positions, such as lower leg [45], waist [8], hip [46], hip pocket, chest pocket and hand [47]. With the prevailing of smartphone, researchers have proposed several gait-based authentication systems by utilizing the built-in accelerometer [48], [4], [49]. In a previous work, the researchers analyzed human gait by a shoe-embedded piezoelectric energy harvester [50]. Weitao et al. [51] proposed an automatic key generation system for on-body devices by using gait.

Studies on KEH: There has been extensive studies on wearable sensors. However, wearable sensors consume power and most existing wearable products are powered by batteries. Therefore, frequent recharge and replacement of the batteries are required, which has become the main obstacle on the way of achieving continuous gait recognition. To overcome this problem, researchers are investigating to use the output signal from KEH to achieve a wide range of applications in activity tracking [15], [52] and health monitoring [53]. In [15], [52], the authors proposed the idea of using the energy harvesting power signal for human activities recognition. Their proposed system can achieve 83% of accuracy for activities recognition. In [53], the authors conducted the first experiment study of using the output voltage signal from the PEH to estimate calorie expenditure of human activities. They have shown promising results of replacing accelerometer using KEH for calorie expenditure. Following this trend of study, the proposed KEH-Gait utilizes the voltage signal generated by the kinetic energy harvester from walking to perform gait recognition. By doing so, KEH-Gait can reduce the power consumption of the gait recognition in the wearable device by not using the accelerometer.

X. Conclusion

In this paper, we explore the feasibility of using KEH to address the problem of user spoofing attacks in emerging mobile healthcare systems. In particular, we present KEH-Gait, a kinetic energy harvesting signal based gait recognition system for user authentication. By not using the accelerometer, the proposed KEH-Gait eliminates the need for powering the accelerometer, making gait recognition practical for future self-powered devices. We design and implement hardware platforms to collect voltage data from two types of KEH, PEH and EEH. Evaluation results based on a dataset of 20 subjects show that, using a novel classification method (MSSRC), KEH-Gait is able to achieve recognition accuracy comparable to accelerometer-based gait recognition. Besides, KEH-Gait improves recognition accuracy by up to 10% compared to several state-of-the-art classification algorithms. More importantly, compared to conventional accelerometer-based gait detection, KEH-Gait can reduce energy consumption by 78.15%. To the best of our knowledge, this is the first work that experimentally validates the feasibility of gait recognition using KEH, and our results show that the output voltage signal of energy harvester is a promising informative signal for wearable authentication system.

References

[1] F. Albinali, S. Intille, W. Haskell, and M. Rosenberger, "Using wearable activity type detection to improve physical activity energy expenditure estimation," in *Proceedings of the International conference on Ubiquitous computing*. ACM, 2010, pp. 311–320.

[2] J. Lester, C. Hartung, L. Pina, R. Libby, G. Borriello, and G. Duncan, "Validated caloric expenditure estimation using a single body-worn sensor," in *Proceedings of the International conference on Ubiquitous computing*. ACM, 2009, pp. 225–234.

[3] M. Rabbi, S. Ali, T. Choudhury, and E. Berke, "Passive and in-situ assessment of mental and physical well-being using mobile sensors," in *Proceedings of the 13th international conference on Ubiquitous computing*. ACM, 2011, pp. 385–394.

[4] Y. Ren, Y. Chen, M. C. Chuah, and J. Yang, "Smartphone based user verification leveraging gait recognition for mobile healthcare systems," in *Sensor, Mesh and Ad Hoc Communications and Networks (SECON), 2013 10th Annual IEEE Communications Society Conference on*. IEEE, 2013, pp. 149–157.

[5] Y. Ren, J. Yang, M. C. Chuah, and Y. Chen, "Mobile phone enabled social community extraction for controlling of disease propagation in healthcare," in *2011 IEEE Eighth International Conference on Mobile Ad-Hoc and Sensor Systems*. IEEE, 2011, pp. 646–651.

[6] D. Cunado, M. S. Nixon, and J. N. Carter, "Automatic extraction and description of human gait models for recognition purposes," *Computer Vision and Image Understanding*, vol. 90, no. 1, pp. 1–41, 2003.

[7] D. Gafurov, K. Helkala, and T. Søndrol, "Gait recognition using acceleration from mems," in *Availability, Reliability and Security, 2006. ARES 2006. The First International Conference on*. IEEE, 2006, pp. 6–pp.

[8] H. J. Ailisto, M. Lindholm, J. Mantyjarvi, E. Vildjiounaite, and S.-M. Makela, "Identifying people from gait pattern with accelerometers," in *Defense and Security*. International Society for Optics and Photonics, 2005, pp. 7–14.

[9] Y. Zhang, G. Pan, K. Jia, M. Lu, Y. Wang, and Z. Wu, "Accelerometer-based gait recognition by sparse representation of signature points with clusters," 2014.

[10] M. Rostami, A. Juels, and F. Koushanfar, "Heart-to-heart (h2h): authentication for implanted medical devices," in *CCS' 2013*. ACM, 2013, pp. 1099–1112.

[11] M. Gorlatova, J. Sarik, G. Grebla, M. Cong, I. Kymissis, and G. Zussman, "Movers and shakers: Kinetic energy harvesting for the internet of things," in *Proceedings of the ACM SIGMETRICS Performance Evaluation Review*, vol. 42, no. 1. ACM, 2014, pp. 407–419.

[12] T. Von Büren, P. D. Mitcheson, T. C. Green, E. M. Yeatman, A. S. Holmes, and G. Tröster, "Optimization of inertial micropower generators for human walking motion," *Sensors Journal, IEEE*, vol. 6, no. 1, pp. 28–38, 2006.

[13] J. Yun, S. N. Patel, M. S. Reynolds, and G. D. Abowd, "Design and performance of an optimal inertial power harvester for human-powered devices," *Mobile Computing, IEEE Transactions on*, vol. 10, no. 5, pp. 669–683, 2011.

[14] P. D. Mitcheson, E. M. Yeatman, G. K. Rao, A. S. Holmes, and T. C. Green, "Energy harvesting from human and machine motion for wireless electronic devices," *Proceedings of the IEEE*, vol. 96, no. 9, pp. 1457–1486, 2008.

[15] S. Khalifa, M. Hassan, and A. Seneviratne, "Pervasive self-powered human activity recognition without the accelerometer," in *Proceedings of the International Conference on Pervasive Computing and Communications*. IEEE, 2015, pp. 79–86.

[16] A. Bilbao, D. Hoover, J. Rice, and J. Chapman, "Ultra-low power wireless sensing for long-term structural health monitoring," *Sensors and Smart Structures Technologies for Civil, Mechanical, and Aerospace Systems (San Diego, California, USA,)*, pp. 798 109–14, 2011.

[17] "AMPY," http://www.getampy.com/ampy-move.html//.

[18] "SOLEPOWER," http://www.solepowertech.com/#new-page//.

[19] "KINERGIZER," http://kinergizer.com/.

[20] F. Lu, H. Lee, and S. Lim, "Modeling and analysis of micro piezoelectric power generators for micro-electromechanical-systems applications," *Smart Materials and Structures*, vol. 13, no. 1, p. 57, 2003.

[21] M. Kim, M. Hoegen, J. Dugundji, and B. L. Wardle, "Modeling and experimental verification of proof mass effects on vibration energy harvester performance," *Smart Materials and Structures*, vol. 19, no. 4, p. 045023, 2010.

[22] J. M. Renno, M. F. Daqaq, and D. J. Inman, "On the optimal energy harvesting from a vibration source," *Journal of sound and vibration*, vol. 320, no. 1, pp. 386–405, 2009.

[23] D. J. Ewins, *Modal testing: theory and practice*. Research studies press Letchworth, 1984, vol. 15.

[24] S. Ravi, A. Raghunathan, and S. Chakradhar, "Tamper resistance mechanisms for secure embedded systems," in *VLSI Design, 2004. Proceedings. 17th International Conference on*. IEEE, 2004, pp. 605–611.

[25] L. Guan, J. Xu, S. Wang, X. Xing, L. Lin, H. Huang, P. Liu, and W. Lee, "From physical to cyber: Escalating protection for personalized auto insurance," in *Sensys*, 2016.

[26] H. Liu, S. Saroiu, A. Wolman, and H. Raj, "Software abstractions for trusted sensors," in *Mobisys*. ACM, 2012, pp. 365–378.

[27] Y. Shen, W. Hu, M. Yang, B. Wei, S. Lucey, and C. T. Chou, "Face recognition on smartphones via optimised sparse representation classification," in *Proceedings of the International Symposium on Information Processing in Sensor Networks*. IEEE, 2014, pp. 237–248.

[28] A. Brajdic and R. Harle, "Walk detection and step counting on unconstrained smartphones," in *Proceedings of the international joint conference on Pervasive and ubiquitous computing*. ACM, 2013, pp. 225–234.

[29] S. Butterworth, "On the theory of filter amplifiers," *Wireless Engineer*, vol. 7, no. 6, pp. 536–541, 1930.

[30] F. Glover and M. Laguna, *Tabu Search*. Springer, 2013.

[31] J. Wright, A. Yang, A. Ganesh, S. Sastry, and Y. Ma, "Robust face recognition via sparse representation," *PAMI*, pp. 210–227, 2009.

[32] W. Xu, Y. Shen, N. Bergmann, and W. Hu, "Sensor-assisted face recognition system on smart glass via multi-view sparse representation classification," in *IPSN*. ACM, 2016.

[33] B. Wei, M. Yang, Y. Shen, R. Rana, C. T. Chou, and W. Hu, "Real-time classification via sparse representation in acoustic sensor networks," in *Proceedings of the 11th ACM Conference on Embedded Networked Sensor Systems*. ACM, 2013, p. 21.

[34] M. Moreau, "Estimating the energy consumption of emerging random access memory technologies," 2013.

[35] F. Büsching, U. Kulau, M. Gietzelt, and L. Wolf, "Comparison and validation of capacitive accelerometers for health care applications," *Computer methods and programs in biomedicine*, vol. 106, no. 2, pp. 79–88, 2012.

[36] S. Enokida, R. Shimomoto, T. Wada, and T. Ejima, "A predictive model for gait recognition," in *2006 Biometrics Symposium: Special Session on Research at the Biometric Consortium Conference*. IEEE, 2006, pp. 1–6.

[37] M. Muaaz and C. Nickel, "Influence of different walking speeds and surfaces on accelerometer-based biometric gait recognition," in *Telecommunications and Signal Processing (TSP), 2012 35th International Conference on*. IEEE, 2012, pp. 508–512.

[38] D. Gafurov and E. Snekkenes, "Gait recognition using wearable motion recording sensors," *EURASIP Journal on Advances in Signal Processing*, vol. 2009, p. 7, 2009.

[39] T. H. Lam and R. S. Lee, "A new representation for human gait recognition: Motion silhouettes image (msi)," in *Advances in Biometrics*. Springer, 2005, pp. 612–618.

[40] A. Kale, A. Sundaresan, A. Rajagopalan, N. P. Cuntoor, A. K. Roy-Chowdhury, V. Krüger, and R. Chellappa, "Identification of humans using gait," *Image Processing, IEEE Transactions on*, vol. 13, no. 9, pp. 1163–1173, 2004.

[41] Z. Liu and S. Sarkar, "Improved gait recognition by gait dynamics normalization," *Pattern Analysis and Machine Intelligence, IEEE Transactions on*, vol. 28, no. 6, pp. 863–876, 2006.

[42] J. Han and B. Bhanu, "Individual recognition using gait energy image," *Pattern Analysis and Machine Intelligence, IEEE Transactions on*, vol. 28, no. 2, pp. 316–322, 2006.

[43] R. J. Orr and G. D. Abowd, "The smart floor: a mechanism for natural user identification and tracking," in *CHI'00 extended abstracts on Human factors in computing systems*. ACM, 2000, pp. 275–276.

[44] L. Middleton, A. Buss, A. Bazin, M. S. Nixon *et al.*, "A floor sensor system for gait recognition," in *Automatic Identification Advanced Technologies, 2005. Fourth IEEE Workshop on*. IEEE, 2005, pp. 171–176.

[45] D. Gafurov, K. Helkala, and T. Søndrol, "Biometric gait authentication using accelerometer sensor," *Journal of computers*, vol. 1, no. 7, pp. 51–59, 2006.

[46] D. Gafurov, E. Snekkenes, and T. E. Buvarp, "Robustness of biometric gait authentication against impersonation attack," in *On the Move to Meaningful Internet Systems 2006: OTM 2006 Workshops*. Springer, 2006, pp. 479–488.

[47] E. Vildjiounaite, S.-M. Mäkelä, M. Lindholm, R. Riihimäki, V. Kyllönen, J. Mäntyjärvi, and H. Ailisto, "Unobtrusive multimodal biometrics for ensuring privacy and information security with personal devices," in *Pervasive Computing*. Springer, 2006, pp. 187–201.

[48] H. Lu, J. Huang, T. Saha, and L. Nachman, "Unobtrusive gait verification for mobile phones," in *Proceedings of the International Symposium on Wearable Computers*. ACM, 2014, pp. 91–98.

[49] C. Nickel, T. Wirtl, and C. Busch, "Authentication of smartphone users based on the way they walk using k-nn algorithm," in *Intelligent Information Hiding and Multimedia Signal Processing (IIH-MSP), 2012 Eighth International Conference on*. IEEE, 2012, pp. 16–20.

[50] J. Zhao and Z. You, "A shoe-embedded piezoelectric energy harvester for wearable sensors," *Sensors*, vol. 14, no. 7, pp. 12 497–12 510, 2014.

[51] W. Xu, G. Revadigar, C. Luo, N. Bergmann, and W. Hu, "Walkie-talkie: Motion-assisted automatic key generation for secure on-body device communication," in *IPSN*. IEEE, 2016, pp. 1–12.

[52] S. Khalifa, M. Hassan, A. Seneviratne, and S. K. Das, "Energy harvesting wearables for activity-aware services," *Internet Computing, IEEE*, vol. 19, no. 5, pp. 8–16, 2015.

[53] G. Lan, S. Khalifa, M. Hassa, and W. Hu, "Estimating calorie expenditure from output voltage of piezoelectric energy harvester-an experimental feasibility study," in *Proceedings of the 10th EAI International Conference on Body Area Networks (BodyNets)*, 2015.